Sensitivity of some optical properties of fractals to the cut-off functions

1995 J. Phys. A: Math. Gen. 28 297

(http://iopscience.iop.org/0305-4470/28/2/008)

J. Phys. A: Math. Gen. 28 (1995) 297–316. Printed in the UK

Sensitivity of some optical properties of fractals to the cut-off functions

Robert Botet†, Pascal Rannou‡ and Michel Cabane‡

† Laboratoire de Physique des Solides, CNRS LA2, Bâtiment 510, Université Paris-Sud Centre d'Orsay, F-91405 Orsay, France

‡ Service d'Aéronomie, Tour 15, Boîte 102, Université de Paris 6, 4 Place Jussieu, 75252, Paris Cedex 05, France

Received 25 July 1994, in final form 31 October 1994

Abstract. In physics, fractal objects are basically finite. This means that their geometrical features must be corrected by natural cut-offs. In the important example of aggregates of small units, the scaling behaviours break down both for small length-scales (reflecting the typical size of the monomers) and for large length-scales (due to the finite extent of the aggregate). These cut-off functions are either ignored in the theoretical studies, or they are modelled by a simple exponential function. In this paper we show that this simple form is not the generic case and that some physical properties depend quantitatively on the precise form of these cut-offs. Explicit analytical and numerical models, mainly connected to the cluster–cluster aggregation model, are studied from this perspective. All of them exhibit roughly the same form of cut-off function. We discuss the sensitivity to these functions of some optical properties of importance in light scattering experiments.

1. Introduction

Let us consider a fractal aggregate of N units. Each unit is assumed to have the same geometrical form and physical properties. For simplicity they may be imagined as balls of identical radius a. The mass-correlations inside one such aggregate are representative of the scale-invariant structure. When one knows the density $\rho(r)$, one simple way to study the morphology of such an object is the density–density correlation function defined by [1]

$$C(r) = \frac{\left\langle \int \rho(r')\rho(r'+r)\,\mathrm{d}^3r' \right\rangle}{\left(\left\langle \int \rho(r')\,\mathrm{d}^3r' \right\rangle \right)^2}. \tag{1}$$

Thereafter, the notation $\langle \cdots \rangle$ indicates the average over a large number of aggregates of the same size. The main property of this correlation function is its power-law behaviour

$$C(r) \sim r^{D-3} \tag{2}$$

for such values of the distance r lying between a and a typical radius of the aggregate, say R. The exponent D is the fractal dimension of the cluster, and is characteristic of its mass distribution. Its value, in the scaling range of r, must be larger than 1 for a connected aggregate and smaller than the dimension of the space (here 3) for non-overlapping units. The Fourier transform of the density–density correlation function has a very simple form, since it separates the contribution of the units from the information on the aggregate [2].

0305-4470/95/020297+20$19.50

More precisely, if one defines the origin of the coordinates, $\boldsymbol{r} = \mathbf{0}$, at the centre of mass, then

$$\widehat{C}(\boldsymbol{k}) = \frac{s^2(\boldsymbol{k})}{N^2}\left|\left\langle \sum_j \mathrm{e}^{\mathrm{i}\boldsymbol{k}\boldsymbol{r}_j}\right\rangle\right|^2 . \tag{3}$$

The factor $s(\boldsymbol{k})$ is the form-factor of one unit, which for a homogeneous ball of radius a is given by

$$s(\boldsymbol{k}) = \frac{3}{k^3a^3}(\sin(ka) - ka\cos(ka)) . \tag{4}$$

Note, in particular, that equation (3) implies some constraints on the correlation function; for example, $\widehat{C}(\boldsymbol{k})$ must be real and non-negative. This gives a strong limitation on the functions which may represent such correlations.

We shall see another correlation function, namely the distance distribution [3]:

$$P(r) = \left\langle \frac{1}{N(N-1)} \sum_{i\neq j} \delta(r - r_{ij}) \right\rangle \tag{5}$$

where the sum is over all the pairs of different units. The vector $\boldsymbol{r}_{ij}$ is the difference $\boldsymbol{r}_i - \boldsymbol{r}_j$, and δ is the Dirac distribution. In other words, this function $P(r)$ denotes the average number of pairs of units whose centres are separated by the distance r. Contrary to the density–density correlation function, there is no information about the internal structure of the units, but simply about the location of their centres. These two functions $C(r)$ and $P(r)$ are linked, as can be seen from their Fourier transforms [2]:

$$\widehat{C}(\boldsymbol{k}) = s^2(\boldsymbol{k})\left(\frac{1}{N} + \left(1 - \frac{1}{N}\right)\widehat{P}(\boldsymbol{k})\right) . \tag{6}$$

From the point of view of the geometrical structure of the aggregate, the density–density correlation function and the distance distribution function contains the same information, but the latter can be more directly physically applicable, e.g. in light scattering phenomena.

Finally, we shall make some general assumptions about the objects to be studied here. One is the statistical isotropy of the objects: that is to say, all the physical quantities which depend on the vector distance $\boldsymbol{r}$ will be assumed to have average values dependent on only the modulus of this vector, r. In particular,

$$P(r)\,\mathrm{d}^3r = 4\pi r^2 P(r)\,\mathrm{d}r \tag{7}$$

and similarly for its Fourier transform. For example, this means that we do not consider the case where anisotropic fractal aggregates are oriented in space because of some external field.

Another general feature of fractals is self-similarity. Because of this property, no typical length can exist in the system except the radius of the monomers, which gives the unit of the lengths, and one global radius of the object, say its radius of gyration R_g:

$$R_g^2 = \langle r^2 \rangle = \frac{1}{2N(N-1)} \sum_{i\neq j} r_{ij}^2 . \tag{8}$$

All the other lengths defined by the system should be expressed in terms of these two quantities. We could also take other definitions of the typical radius of the aggregate (the maximum distance between the units, for example) but the radius of gyration has some advantages: it is easy to define, has small fluctuations around its average value, and occurs

quite naturally in many physical processes. Within this frame, one can write a general approximate form for the average distance distribution in terms of the reduced distances

$$P(r) \simeq \frac{1}{AR_g^3}\left(\frac{r}{R_g}\right)^{D-3} f_{co}\left(\frac{r}{R_g}\right). \tag{9}$$

The cut-off function f_{co} governs the change in the distribution due to the finite extent of the aggregate. Note that we do not take into account the small-length cut-off (for distances smaller than $2a$). This is equivalent to assuming that the radii of the monomers are much smaller than the typical radius of the aggregate. A complete description of the behaviour of the correlation functions near $r = a$ should consider the fine structure of the units, which is not our aim in this paper. Hence, the function f_{co} is essentially equal to 1 when $r \ll R_g$ to recover equation (2), and must vanish for $r > 2(N-1)a$. The numerical coefficient A is expressed by the normalization of the average probability density as

$$A = 4\pi \int_0^\infty x^{D-1} f_{co}(x)\,dx. \tag{10}$$

Because of the definition of the radius of gyration (8), we must have the following constraint on the moments of the function f_{co}:

$$\int_0^\infty x^{D-1}\left(x^2 - 2\right) f_{co}(x)\,dx = 0 \tag{11}$$

which is equivalent to a normalization of the cut-off function.

Finally, since $\widehat{C}(k)$ must be a positive function, the relation (6) constrains the function f_{co} to satisfy the inequality

$$\int_0^\infty x^{D-1} \frac{\sin(\alpha x)}{\alpha x} f_{co}(x)\,dx \geqslant 0 \tag{12}$$

for any real value of the parameter α. As an application of this inequality, one can remark that a step function cannot represent one such cut-off, since (12) fails in this case.

An obvious but important application of the general form of the distance distribution can be found by remarking that there is a proportion $1/N$ of pairs whose mutual distance is equal to $2a$. This means that the integral of $P(r)$ over a ball of radius slightly larger than $2a$ must be equal to $N-1$, or, equivalently

$$N \simeq A'\left(\frac{R_g}{2a}\right)^D. \tag{13}$$

An equation which gives the well known average relation between the number of particles of one cluster and its radius of gyration.

2. General behaviour of the distance distribution function

The Fourier transform of the distribution $P(r)$ can be formally expanded as a series involving average radii:

$$\widehat{P}(k) = \left\langle \frac{2}{N(N-1)} \sum_{i<j} \cos(k \cdot r_{ij}) \right\rangle = \sum_{m=0}^{\infty} (-1)^m a_m (kR_g)^{2m}. \tag{14}$$

The positive quantities a_m which appear in this expansion are defined explicitly as a combination of various averages of the distances of the centres of the units to the centre of

mass (here $\delta_{i,j}$ denotes the Kronecker symbol):

$$a_m = \frac{1}{(2m+1)!} \sum_{s=0}^{\lfloor m/2 \rfloor} \frac{2}{1+\delta_{m,2s}} \left[\sum_{l=0}^{s} \frac{2^{2l}}{2l+1} \binom{m}{2l} \binom{m-2l}{s-l} \right] \frac{\langle (r^2)^s \rangle \langle (r^2)^{m-s} \rangle}{\langle r^2 \rangle^m} . \tag{15}$$

But all these factors, except $a_0 = 1$ and $a_1 = \frac{1}{3}$, are indeed model-dependent. In particular, equation (15) allows one to find the behaviour of $\widehat{P}(k)$ for small values of k:

$$\widehat{P}(k) \simeq \mathrm{e}^{-\frac{1}{3}k^2 R_g^2} . \tag{16}$$

This general Guinier regime is valid as long as $kR_g \ll 1$, but it decreases too sharply, in general. The following corrective term involves the calculation of $\langle (r^2)^2 \rangle / \langle r^2 \rangle^2$ which is yet dependent on the model or on the geometrical structure of the real aggregate. In terms of the distance distribution this regime, for the small values of k in reciprocal space should be related to the behaviour for large values of the distance r in real space, and since the inverse Fourier transform of a Gaussian function like (16) is still a Gaussian function, one could expect the cut-off function of $P(r)$ to be of the same form. Unfortunately, the relation between the distance distribution function and its Fourier transform is not so simple, since it is written as

$$P(r) = \frac{1}{2\pi^2 r} \int_0^\infty k \sin(kr) \widehat{P}(k) \, \mathrm{d}k . \tag{17}$$

The problem arises from the fact that integrals of the form: $k \sin(kr)$ diverge, and the behaviour of (17) at large r is then the consequence of the cancellation of the divergence of the integral of the Fourier transform $\widehat{P}$ at intermediate and large k. Two simple examples clearly demonstrate this phenomenon when r takes positive values:

$$\frac{1}{2\pi^2 r} \int_0^\infty k \sin(kr) \frac{1}{1+\alpha^2 k^2} \, \mathrm{d}k = \frac{1}{4\pi\alpha^2 r} \mathrm{e}^{-r/\alpha} \tag{18}$$

$$\frac{1}{2\pi^2 r} \int_0^\infty k \sin(kr) \, \mathrm{e}^{-\alpha^2 k^2} \, \mathrm{d}k = \frac{1}{8\pi^{3/2}\alpha^3} \mathrm{e}^{-r^2/4\alpha^2} . \tag{19}$$

In these examples, the corresponding functions $\widehat{P}(k)$ behave similarly for small values of k, but decrease quite differently for larger values. The resulting distance distributions, even for large distances, are then completely different.

We shall now focus on a particular type of fractal aggregate of particles, namely the cluster–cluster aggregation (CCA) models [4], which have been shown to be relevant in many areas of physics (colloids, aerosols and polymers, for example). The fundamental particularity of this sort of aggregation is that growth occurs by successive sticking of clusters of comparable sizes. This is quite different from growth where particles are added one after the other on a large cluster. This latter example leads to other classes of universality.

Returning to the cluster–cluster aggregation models, a simple argument allows us to make one conjecture about the asymptotic form of the distance distribution for this example. Let us define the function $Q_N(r)$ as the proportion of pairs of particles (in a cluster of size N) whose relative distance is larger than r. During such a growth two clusters stick to form a larger cluster. We know that we may suppose that the two colliding clusters have exactly the same size N without changing any geometrical feature [5]. Then, the cluster resulting from the aggregation of these two clusters, has size $2N$. We now require the relation between the two functions $Q_{2N}(r)$ and $Q_N(r)$. The pairs of monomers further apart than r, in one given parent cluster of size N, can be found as the two pairs of points

(A, C) and (C, B), where C is any point in the daughter cluster of size $2N$. For large values of r, the two sides AC and CB have lengths comparable to r, which is the length of the side AB. Considering, for simplification, only the equilateral triangles ABC, we get

$$Q_N(r) \sim Q_{2N}^2(r) \tag{20}$$

which leads to a solution of the form $\exp(-f(r)/N)$ for this function. Moreover, here N acts as the typical size of the cluster. Since it is a fractal there is no other length-scale than R_g, and all the distances must be expressed in the scaled form r/R_g, or equivalently r^D/N. The solution we have found for the function $Q_N(r)$ is

$$Q_N(r) \sim e^{-\alpha r^D/N} \tag{21}$$

with some non-dimensional parameter α. This result can be written in terms of the function $P(r)$, since $-4\pi r^2 P(r)$ is just the r-derivative of $Q_N(r)$. This leads to the approximation:

$$P(r) \sim \frac{r^{D-3}}{N} e^{-\alpha r^D/N} \tag{22}$$

which is exactly of the form of (9). To obtain this expression, we have done many crude approximations simply in order to account for the idea of hierarchical growth, but, nevertheless, this gives a precise asymptotic form which we shall try to verify later on some models of this sort. We do not claim here that this is the true distribution in all cases, but simply that this form is a good candidate amongst all imaginable functions in the case of the CCA models. Considering one term after the leading one, we shall write trial distance–distribution cut-off functions more generally as

$$f_{co}(x) \sim \begin{cases} \text{constant} & \text{when} \quad x \to 0 \\ x^{-b} \exp(-cx^D) & \text{when} \quad x \gg 1 \ . \end{cases} \tag{23}$$

In the past, another form for f_{co} has been proposed wherein the large-x behaviour was a simple exponential: $\exp(-x/\xi)$ [6]. This is reminiscent of the Lorentzian form (18) of the Fourier transform. There were at least two reasons for this: first, this form often leads to tractable analytical calculations, which may be very useful. Moreover, this sort of cut-off is present in the correlation functions of systems exhibiting a phase transition [7], and in this case ξ appears as a correlation length. At the critical point, ξ behaves like the total length of the system, so that the problem of the correlation functions seems quite similar both for the fractal aggregates and for the thermodynamic systems at their critical point. However, there is an important difference: the Ornstein and Zernike derivation used to obtain this correlation function is based on the hypothesis that the thermodynamic state of the system is driven by a Landau–Ginzburg free energy, whereas for the fractal aggregates of particles one knows that the evolving system is always far from the equilibrium so that the very definition of some free energy is quite ambiguous for such a system. This makes the Ornstein–Zernike correlation function of doubtful use in our problem.

3. Cut-off functions for some aggregation models

3.1. The overlapping random walk

This model is defined in the following way. A point jumps randomly in ordinary three-dimensional space. Each jump has length $2a$ and random space-orientation, and the set of N successive jumps corresponds to the set of the N centres of the particles of radius $2a$ of the cluster. In this model, overlapping of units is allowed since two non-adjacent

jumping points can be, by chance, at a distance smaller than $2a$. Note, however, that this complication is known to be irrelevant for space-dimension larger than 2.

This model can be solved exactly and the distance distribution is equal to

$$P(r,N)=\frac{1}{N(N-1)\pi^2}\int_0^\infty \frac{\sin(kr)}{kr}\frac{\frac{\sin(2ka)}{2ka}}{\left(1-\frac{\sin(2ka)}{2ka}\right)^2}\times\left[\left(\frac{\sin(2ka)}{2ka}\right)^N-N\frac{\sin(2ka)}{2ka}+N-1\right]k^2\,dk\,. \tag{24}$$

It may be readily developed in a series of Hermite polynomials. The term of order 0 gives the Guinier regime (16) and leads to the radius of gyration (13) with fractal dimension $D=2$ and coefficient $A'=6$. The term of order 1 gives the leading behaviour of the cut-off function f_{co} [8]:

$$f_{co}(x)\sim\begin{cases}4 & \text{when}\quad x\to 0\\ x^{-3}\exp(-x^2/4) & \text{when}\quad x\gg 1\,.\end{cases} \tag{25}$$

Though this is not a CCA model, here we recover the form (23) of the cut-off function with the non-universal values of the parameters $b=3$ and $c=\frac{1}{4}$.

It is of some interest to note that the same sort of cut-off function has been observed in the particle-cluster diffusion-limited aggregation model [9]. In this case, the cluster grows around one seed by addition of randomly landing Brownian particles, so that the centre of mass of the whole aggregate is always close to this initial particle. An analytical mean-field derivation of the average density (the centre of mass being chosen as the centre of the coordinates) leads to a density function of the approximate form

$$\rho(r)\sim\begin{cases}A/r & \text{when}\quad r<R_g\\ B\,e^{-C(r/R_g)^2} & \text{when}\quad r\gg R_g\end{cases} \tag{26}$$

where A, B and C are constants. Replacing the convolution $\rho*\rho$ in definition (1) leads to a Gaussian cut-off function of the form (23), but where the exponent D appearing in the exponential function is replaced by 2 (while the fractal dimension is $D\simeq 2.5$).

3.2. The reaction-limited CCA model

Let us now discuss the CCA models. In these cases the clusters diffuse freely, according to some diffusion law, and they stick when they collide. If the sticking is immediate (at the first collision), this is either the Brownian cluster–cluster aggregation when the diffusion can be simulated by random walks, or the ballistic CCA model if the diffusive trajectories are random lines. They correspond to aggregation in a dense and rarefied fluid medium, respectively, and will be investigated in the next section. Another such model is called the reaction-limited cluster–cluster aggregation [10]. It is defined by a very low sticking probability during a collision. One can show that, under this condition, the precise form of the diffusion is unimportant. The simulations of this model are as follows: at the beginning, one starts with 2^n isolated units which are all considered as clusters of one particle. At a later stage of the simulation, one has obtained a set of larger clusters in the following way: one randomly chooses two clusters of the same size and one particle in each of them. These two particles are placed in contact with one another, the rest of the clusters remaining rigid. Sticking does not occur if some overlapping of other particles is found. If, on the contrary, there is no overlapping, then sticking is effective and thus there is formation of one cluster twice the size. This scheme is continued until there is just one final cluster of size 2^n. This

process is important since it is believed to hold for most of the cluster–cluster aggregation phenomenon where some reversibility occurs. This can be either a small probability of (irreversible) sticking or a reversible sticking. The fractal dimension is found to be equal to $D = 2$ in accordance with the exact result of the at-equilibrium lattice animals model which is believed to be representative of this universality class. More precisely, one finds for the reaction-limited cluster–cluster aggregation model:

$$N \simeq 3.3 \left(\frac{R_g}{2a} \right)^2 \tag{27}$$

for $N < 10^4$ (see figure 1), which is consistent with (13). The following term in the expansion (27) is a constant (independent of R_g) whose order of magnitude is 0.7. The distance distribution function, corrected by this fractal behaviour, is plotted in figure 2 for several sizes, for $N = 256$–4096. The data are well reproduced by one cut-off function of

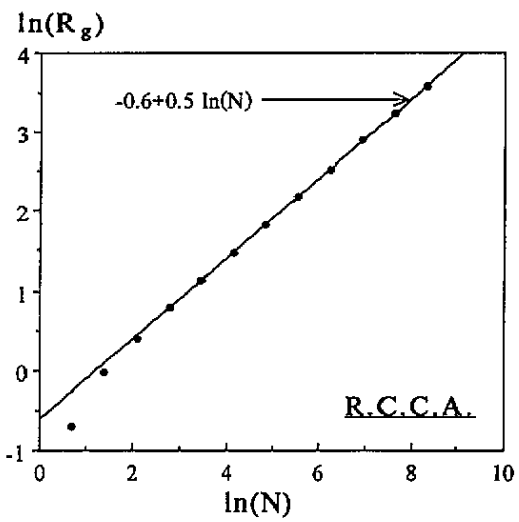

Figure 1. Double-logarithmic plot of the average radius of gyration versus the size of the aggregates, for the three-dimensional off-lattice reaction-limited cluster–cluster aggregation model. Each point corresponds to an average over 1000 independent simulations. The straight line corresponds to (27).

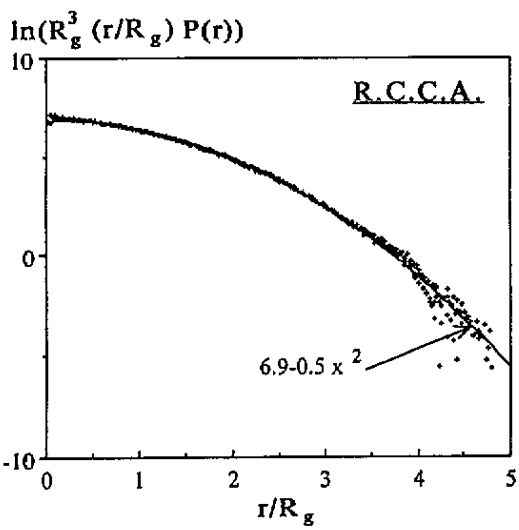

Figure 2. Logarithm of the scaled distance distribution function versus the reduced distances. The crosses are the data for $N = 4096, 2048, 1024, 512$ and 256 units. The scaling (9) is clear. The curve is a best fit (28).

the form (23):

$$f_{co}(x) \sim e^{-x^2/2} \tag{28}$$

with the parameters $b = 0$ and $c = \frac{1}{2}$. Note that this function exactly satisfies constraint (11). We see here that the values of these coefficients are model-dependent, since the random-walk model described above has probably the same value of fractal dimension, but very different values of parameters b and c.

3.3. The Brownian CCA model

This model [11, 12] for rapid aggregation of colloids leads to a fractal dimension of about 1.74 for a number of monomers smaller than 10^4. The relation (13) in this case is written as

$$N \simeq 4.6\left(\frac{R_g}{2a}\right)^{1.74} \tag{29}$$

as can be seen in figure 3. The conjectured form of the cut-off function can be checked by plotting $r^{3-D}P(r)$ versus r^s for various values of the exponent s. This is done on figure 4 for $s = 1$, 1.74 and 2. The best linear behaviour is found for $s = D$ in agreement with the form (23). The large-distance cut-off function of the distance distribution can be approximated well by a law of the form

$$f_{co}(x) \sim \frac{e^{-x^{1.74}/2}}{1 + 0.3x}. \tag{30}$$

This fit is compared in figure 5 with the numerical curves for $N = 256$–4096. If one trusts this cut-off, it verifies (23) with the parameters $b = 1$ and $c = \frac{1}{2}$. The coefficient 0.3 is given by the constraint (11). The uncertainty on the value of b is quite important and here its magnitude should be considered as purely indicative.

3.4. The ballistic CCA model

This is one model for coagulation of aerosols in a rarefied medium. The diffusion of the clusters is modelled by random straight lines in space [13]. The relation between the size

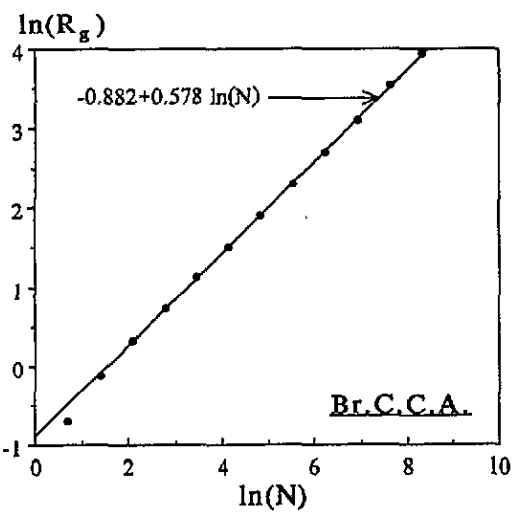

Figure 3. The same as figure 1, for the three-dimensional off-lattice Brownian cluster–cluster aggregation model.

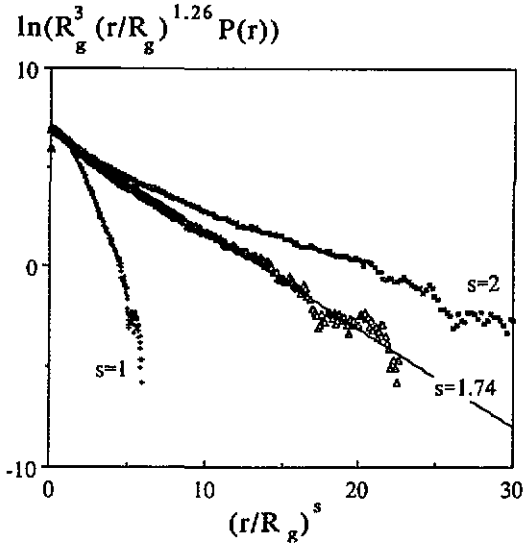

Figure 4. Logarithm of the scaled distance distribution versus the sth power of the reduced distances. The plot is linear near the value $s = D$ (here $D \simeq 1.74$), which is the result given by the argument leading to (22).

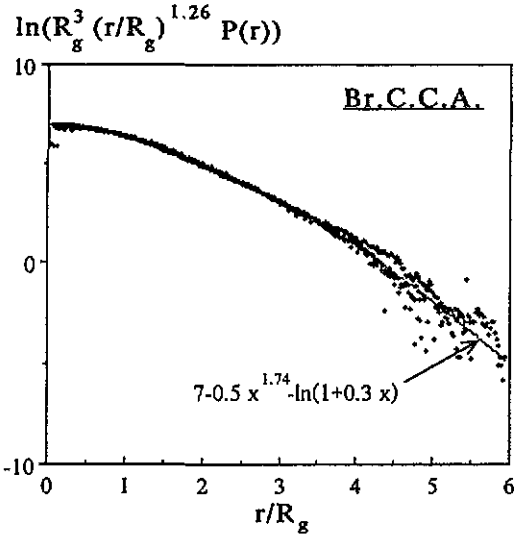

Figure 5. The same as figure 2, for the three-dimensional off-lattice Brownian cluster–cluster aggregation model.

and the radius of gyration is

$$N \simeq 3.9 \left(\frac{R_g}{2a} \right)^{1.90} \tag{31}$$

for cluster sizes smaller than 10^4. This is shown in figure 6. The cut-off function has been studied in the same way as for the reaction-limited and the Brownian CCA model. It can be seen in figure 7 and is approximated well by

$$f_{co}(x) \sim \frac{e^{-x^{1.90}/2}}{1 + 0.03x^2}. \tag{32}$$

The parameters of this law are then found to be $b = 2$ and $c = \frac{1}{2}$. We can note that all the CCA models studied in the present paper lead to the same value of the parameter c, which

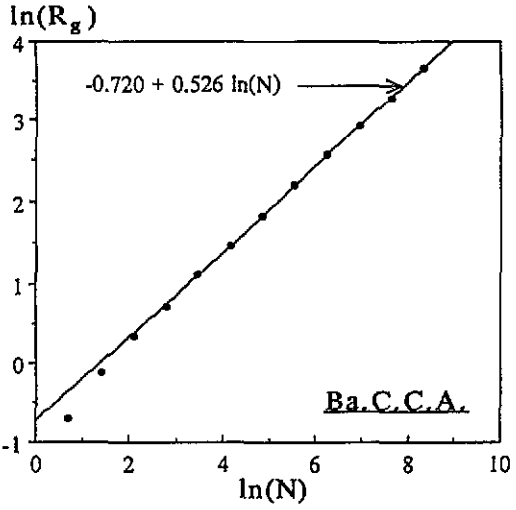

Figure 6. The same as figure 1, for the three-dimensional off-lattice ballistic cluster–cluster aggregation model.

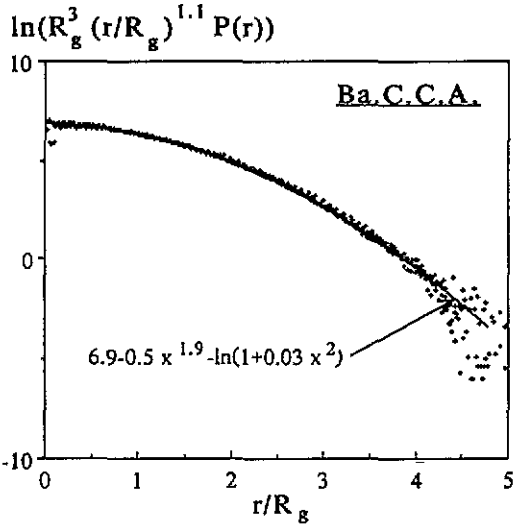

Figure 7. The same as figure 2, for the three-dimensional off-lattice ballistic cluster–cluster aggregation model.

is known with rather good precision (of order 0.03, here) since this is the leading term of f_{co}. The reason for such a coincidence is unknown.

3.5. The compact and linear models

If one fills up the interior of a sphere of radius R with small units of radius a according to the face-centred cubic or the hexagonal close-packed rule, one has

$$N = \left(\frac{20\pi}{9}\sqrt{\frac{10}{3}}\right)\left(\frac{R_g}{2a}\right)^3 \tag{33}$$

since the radius of gyration of such a sphere is equal to $\sqrt{3/5}R$. The Fourier transform of the distance distribution function is approximately equal to the square of the form-factor (4) for one homogeneous ball: $s^2(k)$. Then taking the inverse Fourier transform of this

quantity leads to the exact distibution

$$P(r) = \frac{1}{\frac{4}{3}\pi R^3}\left(1 - \frac{3}{4}\frac{r}{R} + \frac{1}{16}\frac{r^3}{R^3}\right) \tag{34}$$

for $r < 2R$. Of course this function, which counts the distances between units inside one given cluster, must vanish exactly in the case where this distance is larger than $2R$. The above function is in the approximate form (9) with $D = 3$ and a cut-off function

$$f_{co}(x) = \begin{cases} 1 - \dfrac{3\sqrt{3}}{4\sqrt{5}}x + \dfrac{3\sqrt{3}}{80\sqrt{5}}x^3 & \text{when} \quad x < 2\sqrt{\frac{5}{3}} \\ 0 & \text{when} \quad x > 2\sqrt{\frac{5}{3}} \end{cases} \tag{35}$$

which is no longer under the form (23) expected for CCA fractal objects. It shows some similarities with the linear model, where particles are placed linearly, one close to the other. In this case, the radius of gyration is such that

$$\left(\frac{R_g}{2a}\right)^2 = \frac{N^2 - 1}{12} \tag{36}$$

and so (13) holds with $D = 1$ and $A' = \sqrt{12}$. The cut-off function is just equal to

$$f_{co}(x) = \begin{cases} 1 - \dfrac{x}{\sqrt{12}} & \text{when} \quad x < \sqrt{12} \\ 0 & \text{when} \quad x > \sqrt{12}. \end{cases} \tag{37}$$

The latter two examples show, in complement, that the distance distribution cut-off function is not of a universal form in general, even if such a form can exist for some classes of models (e.g. CCA). It is then quite important to study the influence of these non-scaling large-distance behaviours to decide if they change the information which can be extracted from the experimental results. We know that these functions are completely avoided in many cases, and approximated by a simple but probably non-standard form in other cases. Hence, we will continue this work by discussing the influence of the cut-off functions on some physical quantities directly related to light scattering by these fractal objects.

4. Scattering coefficients

We are now interested in physical quantities involving long-range interactions between the units of a same aggregate. A typical example is radiation-scattering experiments.

4.1. The mean-field dipolar approximation

We suppose that light of wavelength λ is scattered by one fractal cluster of N homogeneous spherical units of radius a, much smaller than λ. In this case the electromagnetic field inside each unit is uniform, and can be described by dipolar theory [14]: each particle behaves like a small dipole, and the magnitude of its moment is such that

$$\boldsymbol{p} = 4\pi\epsilon_0 \tfrac{3}{2}\rho \frac{\boldsymbol{E}_{loc}}{k^3} \tag{38}$$

where the vector $\boldsymbol{E}_{loc}$ denotes the local electric field, k is the magnitude of the wavevector ($= 2\pi/\lambda$), and ρ is a function of the p-wave phase shift:

$$\rho = \frac{1}{2i}\left(e^{2i\delta} - 1\right) \qquad \text{with} \qquad \delta \simeq \tfrac{2}{3}(ka)^3 \frac{n^2 - 1}{n^2 + 2}. \tag{39}$$

Its modulus is smaller than 1. The parameter n is the complex refractive index of the units. Each dipole radiates in space an electric field given by

$$\boldsymbol{E} = \frac{k^3}{4\pi\epsilon_0}\frac{e^{ikr}}{kr}\left[\boldsymbol{p}\left(1+\frac{i}{kr}-\frac{1}{k^2r^2}\right)-\boldsymbol{u}(\boldsymbol{u}\boldsymbol{p})\left(1+\frac{3i}{kr}-\frac{3}{k^2r^2}\right)\right] \tag{40}$$

with $\boldsymbol{u}$ being the unit vector in the direction of the distance vector $\boldsymbol{r}$.

In a multiple-scattering approach to this problem, each unit reacts to the incident field (say: $\boldsymbol{E}_{\rm inc} = \boldsymbol{E}_0 e^{i\boldsymbol{k}_{\rm inc}\boldsymbol{r}}$), and to all the other dipolar fields emitted by the other units. One finds then the self-consistent equations [15] for the local fields $\boldsymbol{E}_j$ defined at the centre of the small jth particle:

$$\boldsymbol{E}_j = \boldsymbol{E}_0 e^{i\boldsymbol{k}_{\rm inc}\boldsymbol{r}_j} + \tfrac{3}{2}\rho\sum_{l,l\neq j}\left[\boldsymbol{E}_l\left(1+\frac{i}{kr_{jl}}-\frac{1}{k^2r_{jl}^2}\right)-\boldsymbol{u}_{jl}(\boldsymbol{u}_{jl}\boldsymbol{E}_l)\left(1+\frac{3i}{kr_{jl}}-\frac{3}{k^2r_{jl}^2}\right)\right]\frac{e^{ikr_{jl}}}{kr_{jl}} \tag{41}$$

where we have introduced the relative distance $\boldsymbol{r}_{jl} = \boldsymbol{r}_j - \boldsymbol{r}_l$.

Following Berry and Percival [8], we now introduce the vectorial coefficients $\boldsymbol{d}_j$, similar to electric fields, by

$$\boldsymbol{E}_j = \boldsymbol{d}_j e^{i\boldsymbol{k}_{\rm inc}\boldsymbol{r}_j}. \tag{42}$$

These coefficients are the solutions of an equation very similar to (41). Lastly, we make the mean-field approximation of the d_j-distribution:

$$\boldsymbol{d}_j = \boldsymbol{d}. \tag{43}$$

That is to say: all the units of a same cluster have identical dipolar moments. Because of the linearity of (41), $\boldsymbol{d}$ must be colinear to the incident field $\boldsymbol{E}_0$. Defining the scalar quantity d by $\boldsymbol{d} = d\boldsymbol{E}_0$, equation (41) leads to

$$\frac{1}{d} = 1 - \frac{3\rho}{2}\sum_{l,l\neq j}\left[\left(1+\frac{i}{kr_{jl}}-\frac{1}{k^2r_{jl}^2}\right)-(\boldsymbol{u}_{jl}\boldsymbol{E}_0)^2\left(1+\frac{3i}{kr_{jl}}-\frac{3}{k^2r_{jl}^2}\right)\right]\frac{e^{i(kr_{jl}-\boldsymbol{k}_{\rm inc}\boldsymbol{r}_{jl})}}{kr_{jl}}. \tag{44}$$

This sum, involving only relative distances between monomers of the same cluster, is different over all the units from one given unit (labelled j). When averaging over j, then over a set of independent clusters of same size N, one gets the more tractable formula

$$\frac{1}{d} = 1 - 6\pi\rho(N-1)\int_0^\infty\left[\frac{\sin(kr)}{kr}\left(1+\frac{i}{kr}-\frac{2}{k^2r^2}-\frac{3i}{k^3r^3}+\frac{3}{k^4r^4}\right)+\frac{\cos(kr)}{k^2r^2}\left(1+\frac{3i}{kr}-\frac{3}{k^2r^2}\right)\right]\frac{e^{ikr}}{kr}r^2P(r)\,dr \tag{45}$$

where $P(r)$ is the distance distribution function, as defined in the first section. The foregoing integral is always convergent for $D > 1$, since $P(r) = 0$ when $r > 2a(N-1)$, and the expression in the brackets tends to a constant ($= \frac{11}{15}$) when kr is close to 0.

Once the mean-field value of the dipolar moments are known, all the optical quantities (like the scattering (σ_s), extinction (σ_e) and absorption (σ_a) cross sections, the asymmetry

parameter (g), ...) can readily be calculated [16]:

$$\begin{aligned}
\sigma_e &= \frac{4\pi}{k}\,\mathrm{Im}(f(k_{inc}, k_{inc})E_o)\\
\sigma_s &= \int |f(k_{inc}, k_{sca})|^2\,\mathrm{d}\Omega_s\\
\sigma_a &= \sigma_e - \sigma_s\\
g &= \langle\cos\theta\rangle = \frac{1}{k^2\sigma_s}\int |f(k_{inc}, k_{sca})|^2(k_{inc}k_{sca})\,\mathrm{d}\Omega_s
\end{aligned} \tag{46}$$

with the dipolar field-vector f given by

$$f(k_{inc}, k_{sca}) = \frac{3\rho d}{2k^3}(k_{sca}\times E_o)\times k_{sca}\sum_j \mathrm{e}^{\mathrm{i}(k_{inc}-k_{sca})r_j}\,. \tag{47}$$

More precisely, this leads to the explicit formulae

$$\begin{aligned}
&X = kR_g \qquad \frac{1}{d} = 1 - \rho(I_1(X) + \mathrm{i}I_2(X))\\
&\sigma_e = \frac{6\pi N}{k^2}\,\mathrm{Im}(\rho d) \qquad \sigma_s = \frac{6\pi N}{k^2}|\rho d|^2(1 + I_2(X))\\
&g = \frac{I_3(X)}{1 + I_2(X)}
\end{aligned} \tag{48}$$

where the geometric functions I_1, I_2 and I_3 are given by the following integrals:

$$\begin{aligned}
I_1(X) = \frac{6\pi(N-1)}{A}\int_0^\infty &\left[\frac{\sin(2Xu)}{2(Xu)^2}\left(1 - \frac{5}{(Xu)^2} + \frac{3}{(Xu)^4}\right)\right.\\
&\left.+\frac{\cos(2Xu)}{(Xu)^3}\left(1 - \frac{3}{(Xu)^2}\right)\right]u^{D-1}f_{co}(u)\,\mathrm{d}u
\end{aligned} \tag{49}$$

$$\begin{aligned}
I_2(X) = \frac{6\pi(N-1)}{A}\int_0^\infty &\left[3\frac{(\cos(Xu) - \sin(Xu)/Xu)^2}{(Xu)^4}\right.\\
&\left.+2\frac{\sin(Xu)}{(Xu)^3}\left(\cos(Xu) - \frac{\sin(Xu)}{Xu}\right) + \frac{\sin^2(Xu)}{(Xu)^2}\right]u^{D-1}f_{co}(u)\,\mathrm{d}u
\end{aligned} \tag{50}$$

$$\begin{aligned}
I_3(X) = \frac{6\pi(N-1)}{A}\int_0^\infty &\left[\frac{(\cos(Xu) - \sin(Xu)/Xu)^2}{(Xu)^2}\left(1 - \frac{6}{(Xu)^2} + \frac{45}{(Xu)^4}\right)\right.\\
&-2\frac{\sin(Xu)}{(Xu)^3}\left(\cos(Xu) - \frac{\sin(Xu)}{Xu}\right)\left(1 - \frac{15}{(Xu)^2}\right) + \left.5\frac{\sin^2(Xu)}{(Xu)^4}\right]\\
&\times u^{D-1}f_{co}(u)\,\mathrm{d}u
\end{aligned} \tag{51}$$

which are none other than Fourier transforms of some complicated functions. Let us now discuss in detail the dependence of these integrals on parameter X, and on cut-off function f_{co}. To simplify the following results, we shall use the values of the scattering coefficients for one unit, namely:

$$\sigma_e(1) = \frac{6\pi}{k^2}\,\mathrm{Im}\{\rho\} \qquad \sigma_s(1) = \frac{6\pi}{k^2}|\rho|^2 \qquad \sigma_a(1) = \frac{6\pi}{k^2}\left(\mathrm{Im}\{\rho\} - |\rho|^2\right). \tag{52}$$

4.2. Small-X behaviour

To study the small-X features of these optical quantities, or even for numerical computation, it is often more convenient to rewrite the integrals (49)–(51) in terms of the following regular series:

$$I_1(X) = \frac{6\pi(N-1)}{A}\sum_{l=0}^{\infty}(-1)^l \frac{(l+1)(l+2)\left(4l^2+8l+11\right)}{(2l+5)!}2^{2l+2}X^{2l-1} \times \int_0^{\infty} u^{D+2l-2} f_{co}(u)\,du \tag{53}$$

$$I_2(X) = \frac{6\pi(N-1)}{A}\sum_{l=0}^{\infty}(-1)^l \frac{(2l+3)(2l+5)\left(l^2+3l+4\right)}{(2l+6)!}2^{2l+3}X^{2l} \times \int_0^{\infty} u^{D+2l-1} f_{co}(u)\,du \tag{54}$$

$$I_3(X) = \frac{6\pi(N-1)}{A}\sum_{l=1}^{\infty}(-1)^{l+1} \frac{l(2l+3)(2l+5)(2l+7)\left(l^2+5l+10\right)}{(2l+8)!}2^{2l+4}X^{2l} \times \int_0^{\infty} u^{D+2l-1} f_{co}(u)\,du \tag{55}$$

which simply require knowledge of the values of the f_{co}-moments. Moreover, the numerical calculation of the intermediate quantities I_1, I_2 and I_3 are often much easier using the above series rather than the definitions (49)–(51).

We can remark, in particular, that the leading term of $I_1(X)$ depends on the form of the cut-off function, and that this is recovered in the optical cross sections (but not for g, which depends only on I_2 and I_3)

$$\begin{aligned}
\sigma_e(N) &\simeq N\sigma_e(1)\left(1+(N-1)\frac{|\rho|^2}{\mathrm{Im}\{\rho\}}\right)\left(1+2\,\mathrm{Re}\{\rho\}\alpha\frac{N-1}{kR_g}\right)\\
\sigma_s(N) &\simeq N^2\sigma_s(1)\left(1+2\mathrm{Re}\{\rho\}\alpha\frac{N-1}{kR_g}\right)\\
\sigma_a(N) &\simeq N\sigma_a(1)\left(1+2\mathrm{Re}\{\rho\}\alpha\frac{N-1}{kR_g}\right)\\
g &\simeq \frac{4}{15}\left(1-\frac{1}{N}\right)(kR_g)^2
\end{aligned} \tag{56}$$

with the numerical parameter α—which depends on the cut-off—given by

$$\alpha = \frac{11}{10}\frac{\int_0^{\infty} u^{D-2} f_{co}(u)\,du}{\int_0^{\infty} u^{D-1} f_{co}(u)\,du}. \tag{57}$$

This small-X behaviour holds in the limit $R_g \ll \lambda$, which is a very common case.

4.3. Large-X behaviour

When we do not take into account the cut-off function $f_{co}(u)$ (i.e. when it is made equal to 1), the integrals (50) and (51) are divergent. However, since the main part of the value of these integrals is due to the values of the integrand between 0 and a value of u of order 1, one can easily find the following asymptotics:

$$I_1(X) \simeq J_1\frac{N}{X^D} \tag{58}$$

with

$$J_1 = \frac{6\pi}{2^{D-1}A}\int_0^\infty \left(\frac{\sin u}{u^2}\left(1-\frac{20}{u^2}+\frac{48}{u^4}\right)+\frac{4\cos u}{u^3}\left(1-\frac{12}{u^2}\right)\right)u^{D-1}\,\mathrm{d}u$$

where J_1 is finite for all values of the fractal dimension between 1 and 3. Moreover, the value of AJ_1 is exactly equal to $3\pi^2/2$ when $D = 2$.

If $D < 2$:

$$I_2(X) \simeq J_2\frac{N}{X^D} \tag{59}$$

with

$$J_2 = \frac{6\pi}{A}\int_0^\infty \left[3\frac{(\cos u - \sin u/u)^2}{u^4}+2\frac{\sin u}{u^3}\left(\cos u - \sin u/u\right)+\frac{\sin^2(u)}{u^2}\right]u^{D-1}\,\mathrm{d}u\,.$$

If $D = 2$:

$$I_2(X) \simeq \frac{3\pi}{A}N\frac{\ln(X)}{X^2}\,.$$

If $D > 2$:

$$I_2(X) \simeq \frac{3\pi}{(D-2)A}\frac{N}{X^2}\,.$$

If $D < 2$:

$$I_3(X) \simeq J_3\frac{N}{X^D} \tag{60}$$

with

$$J_3 = \frac{6\pi}{A}\int_0^\infty \left[\frac{(\cos u - \sin u/u)^2}{u^2}\left(1-\frac{6}{u^2}+\frac{45}{u^4}\right)\right.$$
$$\left.-2\frac{\sin u}{u^3}\left(\cos u - \frac{\sin u}{u}\right)\left(1-\frac{15}{u^2}\right)+5\frac{\sin^2(u)}{u^4}\right]u^{D-1}\,\mathrm{d}u\,.$$

If $D = 2$:

$$I_2(X) \simeq \frac{3\pi}{A}N\frac{\ln(X)}{X^2}\,.$$

If $D > 2$:

$$I_2(X) \simeq \frac{3\pi}{(D-2)A}\frac{N}{X^2}\,.$$

An important feature must be remarked here: we see a different behaviour for the fractal dimension D smaller or larger than 2. This has been noted by Berry and Percival [8] with the exponential cut-off, but, as expected, it is quite general. More precisely, one finds when $a \ll \lambda \ll R_g$ three behaviours depending on the value of D. If $1 < D < 2$,

$$\sigma_e(N) \simeq N\sigma_e(1)\frac{A'J_2}{(2ka)^D} \tag{61}$$

$$\sigma_s(N) \simeq N\sigma_s(1)\frac{A'J_2}{(2ka)^D} \tag{62}$$

$$\sigma_a(N) \simeq N\sigma_a(1) \tag{63}$$

$$g \simeq \frac{J_3}{J_2}\left(1-\frac{(2ka)^D}{A'J_2}\right). \tag{64}$$

If $D = 2$, the following formulae hold:

$$\sigma_e(N) \simeq N\sigma_e(1)\frac{3\pi A'}{8A}\frac{\ln(4k^2a^2N/A')}{k^2a^2} \tag{65}$$

$$\sigma_s(N) \simeq N\sigma_s(1)\frac{3\pi A'}{8A}\frac{\ln(4k^2a^2N/A')}{k^2a^2} \tag{66}$$

$$\sigma_a(N) \simeq N\sigma_a(1) \tag{67}$$

$$g \simeq 1 - \frac{8Ak^2a^2}{3\pi A'\ln(4k^2a^2N/A')} \tag{68}$$

and, lastly, if $D > 2$, one has

$$\sigma_e(N) \simeq N\sigma_e(1)\frac{3\pi A'^{2/D}}{4(D-2)A}\frac{N^{1-2/D}}{k^2a^2} \tag{69}$$

$$\sigma_s(N) \simeq N\sigma_s(1)\frac{3\pi A'^{2/D}}{4(D-2)A}\frac{N^{1-2/D}}{k^2a^2} \tag{70}$$

$$\sigma_a(N) \simeq N\sigma_a(1) \tag{71}$$

$$g \simeq 1 - \frac{4(D-2)Ak^2a^2}{3\pi A'^{2/D}N^{1-2/D}}. \tag{72}$$

Note the very simple behaviour of the absorption cross section, which is simply, at first approximation, the sum of the absorption cross sections of the N individual units, even for multiple scattering†.

Having given the general small-X and large-X behaviours, we shall now take two examples among the possible cut-off functions, and study the magnitudes of the optical cross sections in the whole range of values of X. Let us take the reaction-limited CCA model ($D = 2$) successively with the following trial cut-offs:

$$\text{Exercise 1:} \quad f_{co}(x) = e^{-x^2/2} \tag{73}$$

$$\text{Exercise 2:} \quad f_{co}(x) = e^{-x\sqrt{3}}. \tag{74}$$

The first example is just the solution (28) found numerically for this model. It should yield the correct answer. The second one is a simple exponential function which also satisfies the constraint (11).

4.4. The correct cut-off (exercise 1)

In this case the normalization coefficient A is equal to 4π, by definition (10), the coefficient A' is 3.3 by (27), and the moments of the cut-off function are given by:

$$\int_0^\infty u^{D+s} f_{co}(u)\,du = 2^{(s+1)/2}\Gamma\left(\frac{s+3}{2}\right). \tag{75}$$

† This result for the absorption cross section, and the behaviour of σ_s in the case of the exponential cut-off with the choice $A' = (2\sqrt{2})^D$, has been given previously by Berry and Percival [8].

With these simple results, the expressions (53)–(55) can be written simply as

$$I_1(X) = \frac{3}{2}\sqrt{\frac{\pi}{2}}\frac{N-1}{X}\sum_{l=0}^{\infty}\frac{4l^2+8l+11}{(2l+1)(2l+3)(2l+5)}\frac{(-2X^2)^l}{l!} \tag{76}$$

$$I_2(X) = 3(N-1)\sum_{l=0}^{\infty}\frac{l^2+3l+4}{(l+2)(l+3)}\frac{l!}{(2l+2)!}(-8X^2)^l \tag{77}$$

$$I_3(X) = 24(N-1)X^2\sum_{l=0}^{\infty}\frac{(l+1)(l^2+7l+16)}{(l+3)(l+4)(l+5)}\frac{(l+1)!}{(2l+4)!}(-8X^2)^l \tag{78}$$

which are uniformly convergent series for all values of the parameter X.

4.5. The exponential cut-off (exercise 2)

When replacing the function (74) in the integrals (49)–(51), and knowing $A = 4\pi/3$ and $A' = 3.3$, one finds the rather simple formulae

$$I_1(X) = \frac{9}{4}\frac{N-1}{X^2}\left(\left(1+\frac{3}{2X^2}+\frac{9}{8X^4}\right)\tan^{-1}\left(\frac{2X}{\sqrt{3}}\right)-\frac{2}{X\sqrt{3}}\left(1+\frac{9}{8X^2}\right)\right) \tag{79}$$

$$I_2(X) = \frac{9}{8}\frac{N-1}{X^2}\left(\left(1+\frac{3}{2X^2}+\frac{9}{8X^4}\right)\ln\left(1+\frac{4X^2}{3}\right)-\left(1+\frac{3}{2X^2}\right)\right) \tag{80}$$

$$I_3(X) = \frac{9}{8}\frac{N-1}{X^2}\left(\left(1+\frac{3}{2X^2}\right)\left(1+\frac{3}{2X^2}+\frac{9}{8X^4}\right)\ln\left(1+\frac{4X^2}{3}\right)-\left(\frac{7}{3}+\frac{3}{X^2}+\frac{9}{4X^4}\right)\right). \tag{81}$$

4.6. Comparing these different cut-offs

The small-X behaviours in the two preceding cases show that the leading terms of $I_1/(N-1)$ are slightly different in the two cases under consideration—$1.378/X$ for the first cut-off (73), and $1.905/X$ for (74)—but their orders of magnitude are comparable. For I_2 and I_3, the leading terms are similar. Hence, we do not expect strong differences in the optical quantities when the wavelength is much larger than the radius of gyration of the aggregate. However, in principle, the above derivations should be valid, in this mean-field dipolar approximation, for $ka \ll 1$, which is a much weaker condition. With $n = 1.5$ and $\lambda/a = 25$ chosen as a standard and quite ordinary set of parameters, the reduced scattering cross sections $(\sigma_s(N)/(\pi a^2))$ are plotted in figure 8 for these two cut-off functions, as a function of the size, and the asymmetry parameter g in figure 9 as a function of the logarithm of the size of the clusters. Since n is real, the absorption cross section σ_a must vanish, and so the extinction and scattering cross sections must coincide, as we can easily verify in the above formulae (since $|\rho|^2 = \mathrm{Im}\{\rho\}$, in this case).

Since, $kR_g \simeq 0.2767\sqrt{N}$, the small-$X$ behaviour coincides here with the range $N \ll 13$, and effectively, the two sets of values are very similar in this case. Moreover, they are well represented by the small-X formulae (56). However, for this numerical example, we see that the results for the two cut-off functions are rather different as soon as the size N is no longer small. Let us look more closely at the $N = 128$ results, for example. The correct cut-off leads to a scattering cross section equal to 0.6314, while the exponential cut-off gives a value some 50% larger ($\sigma_s = 1.0488$). The large-X behaviour is beyond the plotted range of X. Notice, however, that the formulae (65) yield a ratio between the two scattering sections approaching the value 3 when X becomes infinite.

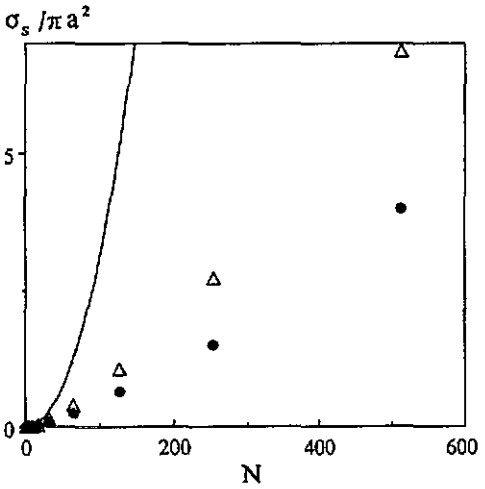

Figure 8. Plot of the reduced scattering cross section versus the size of the aggregates, in the mean-field dipolar theory of the multiple light-scattering. The parameters are $n = 1.5$, $\lambda = 25a$, and the model is the reaction-limited cluster–cluster aggregation. Full circles are the results for the correct cut-off function shown in figure 2. Triangles are the data for the exponential cut-off function (74). The full curve is the small-X behaviour, as approximated by (56).

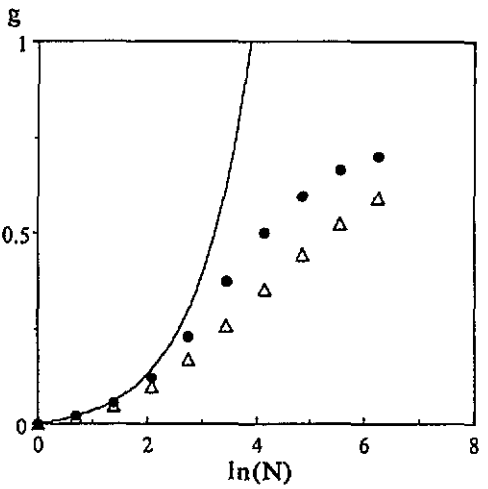

Figure 9. Plot of the asymmetry parameter versus the logarithm of the size of the aggregates. Same optical parameters and same notations as for figure 8.

The same sort of remarks can be made for the asymmetry parameter. The values are 0.5964 and 0.4449, respectively, for $N = 128$, i.e. a relative difference of some 30%. When one knows the importance of the influence of the magnitude of these quantities on some optical properties (e.g. the albedo of planetary atmospheres), one concludes that it is quite important to be careful about cut-off functions in order to obtain reasonable values for optical observables. In particular, chapter 3 provides a list of correct approximations of the large-scale cut-off functions for the Brownian, ballistic and chemical cluster–cluster aggregation models, to be used in the calculation of some optical quantities.

5. Conclusion

If one is only interested in the angular distribution of the intensity of the light scattered by such fluffy aggregates, one has simply to determine the range in the moment transfer ($q = 4\pi \sin(\theta/2)/\lambda$) which corresponds to the scaling.

In this case, it is not important to take the cut-off functions into account, since one only deals only with the self-similar part of the aggregate. On the contrary, many physical applications need precise values of the optical cross sections, and not just some scaling behaviours. These quantities are directly related to some average of the scattered or absorbed intensity, this average being performed over the scaling but also the non-scaling range of the parameters. Let us take the scattering cross section, for example. It is the average of the scattered intensity of the light over all the angles θ. In a wide range of values of θ, the system looks like a perfect self-similar structure, since the inverse of q is much larger than a and much smaller than R_g. However, if the scattering angle is too small, the system is no longer in the self-similar regime. Nevertheless this still has to be counted in the average

for the calculation of this cross section. The present work has been devoted to answering the question of whether this non-scaling part is important or not.

We then investigated the influence of these cut-offs between the scaling and the non-scaling regimes in the mean-field dipolar approximation for scattering. The conclusion is that, generally, the optical cross sections depend quantitively on the cut-off functions. This effect is particularly important when the wavelength λ is smaller than, or of the same order of magnitude of, R_g (i.e. large values of X). In this case, the presence of the factor A in (59), (65) and (69) can completely change the order of magnitude of the optical quantities. However, even in less extreme cases, for example if the size parameter X is not very large, the effect of the cut-off is still evident (see the discussion of the point $N = 128$ of figures 8 and 9, which corresponds to $X = 3.1$). In this case, the form of the cut-off in the distance distribution functions plays a role, and a correct form must be taken in the calculations to get correct numerical values of the cross sections. Another general feature found here is that the larger the size of the aggregate, the more important is the sensitivity to the cut-offs. This dependence can be qualitatively explained using the following argument: the optical cross sections are derived here as Fourier transforms of some functions of the distance, but if the distances are allowed to go to infinity, these integrals diverge. It is then not surprising that the cut-offs in the distances have a great influence on the numerical value of these Fourier transforms, and hence on the optical quantities. The effect is more important for large clusters because the distances to be taken into account are large, and the divergence of the integrals takes place for infinite distances.

In this paper, we also give explicitly the analytical expressions for the scattering, extinction, absorption cross sections, as well as the asymmetry parameter, in terms of the cut-off function. These cut-off functions have been computed for the most common cluster–cluster aggregation models, which are important in the physics of aerosols, colloids and polymers, and they have never been found equal to a simple exponential cut, as had been proposed previously. We can now use the formulae (28), (30), (32), (48), and (53)–(55) as recipes to compute reasonable values of the optical cross sections of fractal aggregates in a number of cases.

Acknowledgment

We are grateful to Seán Gough for essential linguistic help.

References

[1] Witten T A and Sander L M 1981 *Phys. Rev. Lett.* **47** 1400
[2] Guinier A and Fournet G 1955 *Small Angle Scattering of X-Rays* (New York: Wiley)
[3] Axelos M A V, Tchoubar D and Jullien R 1986 *J. Physique* **47** 1843
[4] Botet R and Jullien R 1990 *Phase Transitions* **24–26** 691
Meakin P 1992 *Phys. Scr.* **46** 295
[5] Botet R, Jullien R and Kolb M 1984 *J. Phys. A: Math. Gen.* **17** L75
[6] Sinha S K, Freltoft T and Kjems J 1984 *Kinetics of Aggregation and Gelation* ed F Family and D P Landau (Amsterdam: Elsevier)
Chen Sow-Hsin and Teixeira J 1986 *Phys. Rev. Lett.* **57** 2583
[7] Munster A 1966 *Fluctuation Phenomena in Solids* ed R E Burgess (New York: Academic)
[8] Berry M V and Percival I C 1986 *Opt. Acta* **33** 577
[9] Racz Z and Vicsek T 1983 *Phys. Rev. Lett.* **51** 2385
[10] Jullien R and Kolb M 1984 *J. Phys. A: Math. Gen.* **17** L639
Meakin P and Family F 1987 *Phys. Rev.* A **36** 5498
[11] Meakin P 1993 *Phys. Rev. Lett.* **51** 1119

[12] Kolb M, Jullien R and Botet R 1993 *Phys. Rev. Lett.* **51** 1123
[13] Meakin P 1984 *J. Colloid Interf. Sci.* **102** 205
[14] Van de Hulst H C 1957 *Light Scattering by Small Particles* (New York: Wiley)
[15] Jones A R 1979 *Proc. R. Soc.* A **366** 111
[16] Bohren C and Huffman D 1983 *Absorption and Scattering of Light by Small Particles* (New York: Wiley)